Supplementary Materials for:

"Effects of Fe, Si, Cu, and TiB_2 grain refiner amounts on the hot tearing susceptibility of 5083, 6061, and 7075 aluminum ingots"

Kai-Yu LIANG[1], Hao-Chuan HUANG[1], Ching-Yao TSENG[1], Mien-Chung CHEN[2], Sheng-Long LEE[2], Chi-Cheng LIN[3], Te-Cheng SU[1*]

[1] Department of Materials Science and Engineering, National Taiwan University, Taipei, Taiwan

[2] Institute of Materials Science and Engineering, National Central University, Taoyuan, Taiwan

[3] Iron and Steel Research and Development Department, China Steel Corporation, Kaohsiung, Taiwan

Supplementary Material 1: uneven thermal stress distribution in CRC mold

Several studies on solidifying alloys in CRC molds [1-3] observed a notable temperature differential near the junction where the sprue and horizontal rod meet (Figure S1). The sprue and rod exhibit a relatively uniform temperature distribution, but the sprue consistently has a higher temperature than the rod. The temperature variations at the junction between the sprue and rod result in significant thermal strains, leading to the formation of hot tears. Simulation results also indicated that the middle of the rod experiences the lowest temperature variations, resulting in the lowest thermal stress.

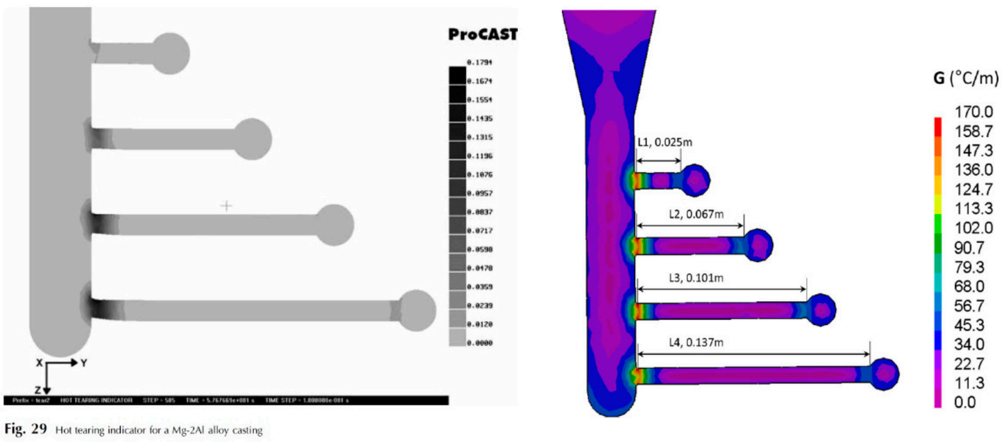

Figure S1. Fields of temperature gradient and HTS indicator discussed in refs. [2,3].

Supplementary Material 2: the difference between Scheil and equilibrium solidification simulations for multicomponent aluminum alloys

Because the cooling conditions did not meet the equilibrium solidification (i.e., the infinite diffusion coefficient of solutes in the primary αAl phase) while casting, the Scheil model was utilized for discussion. This approach can be referenced in the literature [4,5]. The comparison between equilibrium solidification and Schiel solidification for a multicomponent aluminum alloy is shown in Figure S2.

It is worth emphasizing that under typical gravity-casting cooling rates of 1 - 10 K/s, many intermetallic compounds (IMCs) forming only under non-equilibrium solidification conditions can be detected. Examples include Mg_2Si in 6061 aluminum alloy and $Mg(Zn,Cu,Al)_2$ in 7075 aluminum alloy.

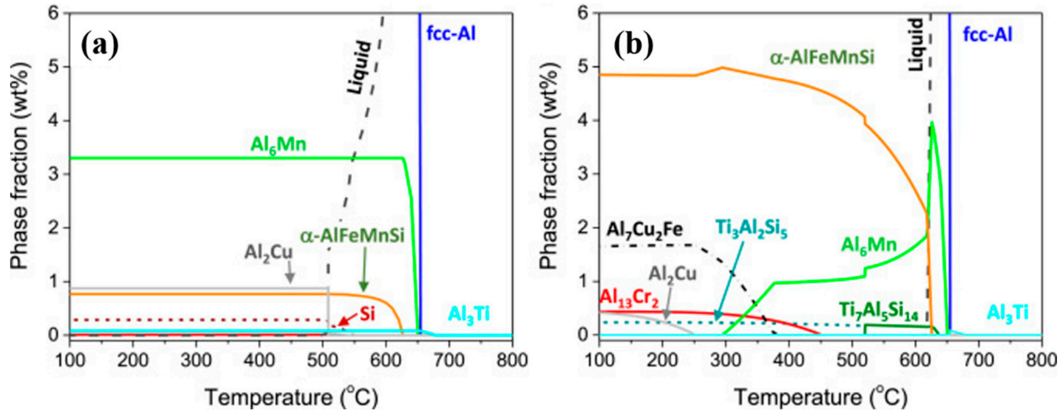

Figure S2. Variation in phase fraction with temperature of A3527 core alloy under (a) Scheil and (b) equilibrium conditions. [5]

Supplementary Material 3: the evidence of inherently brittle fishbone-shaped IMCs

Figure S3 shows that in the 5083 alloys, fishbone-shaped IMCs (α-$Al_{15}(Fe,Mn)_3Si_2$) tend to be brittle and may block interdendritic spaces, making them potential nucleation points for hot tearing.

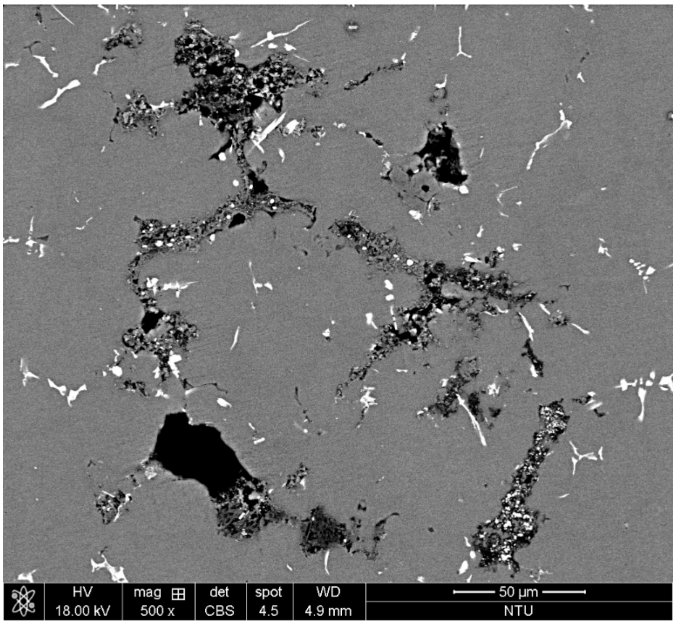

Figure S3. This image is from the magnification of 500x in Figure 5(f), where the fishbone structure IMCs appears fractured.

Supplementary Material 4: the relationship between Al_3Mg_2 and hot tearing in 5083 alloys

Based on Scheil prediction and experimental observations, Al_3Mg_2 forms in Mg-enriched interdendritic liquid with the formation temperature very close to non-equilibrium solidus. As shown in Figure S4, Al_3Mg_2 appears at interdendritic space and may become channels of hot tearing propagation. We can also observe from Figure S4 that Al_3Mg_2 would form between α-$Al_{15}(Fe,Mn)_3Si_2$. Once α-$Al_{15}(Fe,Mn)_3Si_2$ is torn by thermal stress, the crack may propagate through Mg-enriched interdendritic liquid or a continuous Al_3Mg_2.

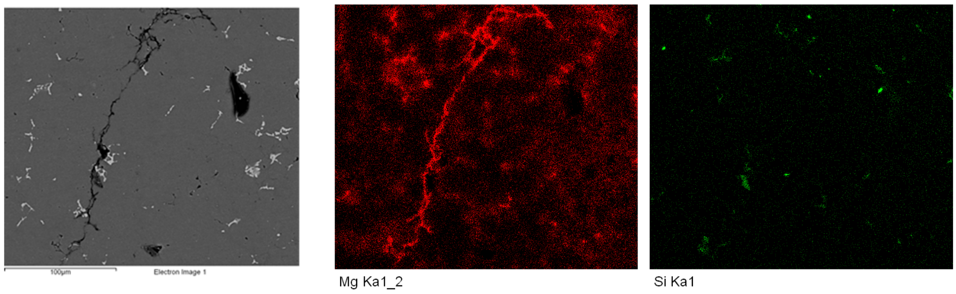

Figure S4. EDS data of 5b From the Si mapping, we could identify that the gray IMCs were Al_3Mg_2 rather than Mg_2Si and can become channels of hot tearing propagation.

Reference:

1. Li, Y.; Li, H.; Katgerman, L.; Du, Q.; Zhang, J.; Zhuang, L. Recent advances in hot tearing during casting of aluminium alloys. *Prog. Mater. Sci.* **2021**, *117*, 100741. https://doi.org/10.1016/j.pmatsci.2020.100741.
2. Cao, G.; Kou, S. Hot cracking of binary Mg–Al alloy castings. *Mater. Sci. Eng. A* **2006**, *417*, 230–238. https://doi.org/10.1016/j.msea.2005.10.050.
3. Wang, K.; Fu, P.; Peng, L.; Wang, Y.; Ding, W. A simplified hot-tearing criterion for shape castings based on temperature-field simulation. *Metall. Mater. Trans. A* **2019**, *50*, 5271–5280. https://doi.org/10.1007/s11661-019-05408-5.
4. Wahlmann, B.; Leidel, D.; Markl, M.; Körner, C. Numerical alloy development for additive manufacturing towards reduced cracking susceptibility. *Crystals* **2021**, *11*, 902. https://doi.org/10.3390/cryst11080902.
5. Jung, J.G.; Cho, Y.H.; Lee, J.M.; Kim, H.W.; Euh, K. Designing the composition and processing route of aluminum alloys using CALPHAD: Case studies. *CALPHAD* **2019**, *64*, 236–247. https://doi.org/10.1016/j.calphad.2018.12.010.